EXPERIMENTAL STUDY ON HEAT TRANSFER CHARACTERISTICS OF HIGH-TEMPERATURE HEAT PIPE

by

Bowen XU[a], Jinwang LI[a,b*], Ningxiang LU[a], and Changji WANG[a]

[a]College of Astronautics, Nanjing University of Aeronautics and Astronautics, Nanjing, China
[b]Jiangsu Province Key Laboratory of Aerospace Power System, Nanjing, China

Original scientific paper
https://doi.org/10.2298/TSCI220207118X

High-temperature heat pipes have broad application prospects in terms of thermal protection of hypersonic aircraft and cooling of space nuclear reactors. In this paper, a high-temperature heat pipe heat transfer performance experimental platform is built to study the heat transfer performance of high-temperature heat pipes at different inclination angles. A heat transfer network model of high-temperature heat pipes containing NCG is established to analyze the influence of NCG. The results show that as the inclination angle of the heat pipe increases, the start-up time of the heat pipe does not change. The heat transfer performance is best when the inclination angle is 30°. High-temperature heat pipes containing NCG will reduce the effective length of the high-temperature heat pipe, increase the thermal resistance, and reduce the heat transfer performance. The high-temperature heat pipe analysis model with NCG established in this paper can be used to predict the heat transfer performance of high-temperature heat pipes containing NCG.

Key words: *high-temperature heat pipe, heat transfer, inclination angle, heating power, NCG*

Introduction

High-temperature heat pipes are one of the hot research directions in the field of heat pipes, and they have broad application prospects in terms of thermal protection of hypersonic aircraft, cooling of space nuclear reactors and solar energy utilization [1-3]. However, due to the high working temperature of high-temperature heat pipes, its working fluid, wick, and pipe materials have certain special characteristics. Some of the existing laws and properties in medium and low-temperature heat pipes may no longer be applicable to high-temperature heat pipes. The experimental conditions of heat pipes are relatively harsh and there are still insufficient researches on the performance of high-temperature heat pipes.

There are some basic heat pipe experiments: Werner *et al*. [4] explored the monel/water heat pipes as an option for operation up to 300 °C. Life tests of up to 30000 hours have shown good compatibility at 250 °C. Xu *et al*. [5] investigated the dynamic response of pulsating heat pipes and the results shows that the dynamic response time constant of pure fluids decreases when the quantity of the liquid working fluid in the pulsating heat pipe de-

*Corresponding author, e-mail: ljw@nuaa.edu.cn

creases with the increase in heating power. Chidambaranathan and Rangaswamy [6] investigate the heat transfer performance of pulsating heat pipe using self-rewetting fluids of high carbon alcohols. The latent heat of vaporization plays an important role in the heat transfer performance of pulsating heat pipe. It was observed that the high carbon alcohols showed a decrease in the latent heat of vaporization. Sun *et al*. [7] according to the thermodynamic model established the heat generation model and coupled heat transfer model of the battery with multi-stage heating method based on flat heat pipes. Different heating powers are assigned to different heating points and the total heating power is kept constant. Mahdavi *et al*. [8] investigated the effect of the working fluid fill volume, inclination angle, and heat input on the equivalent thermal resistance of the heat pipe. Yu *et al*. [9] investigated the start-up performance of high-temperature heat pipe through experiments and the results show that the inclination angle has an obvious influence on the start-up characteristics of high-temperature heat pipe. When the heat pipe is placed horizontally, the temperature rise rate of the heat insulation part *lags*. Li *et al*. [10] carried out an experimental study on the specific structure of the high-temperature heat pipe. The results show that the higher the input power, the shorter the start-up time of the high-temperature heat pipe and the inclination angle of the heat pipe has little effect on the starting performance. The inclination angle increases from 0° to 90° and the steam flow transition temperature of the heat pipe is the same, the start-up time is the same, and the equilibrium temperature is the same. Shen *et al*. [11] carried out experimental research on heat transfer characteristics of high-temperature heat pipe with special structure under different heating conditions. The results show that the starting time and temperature of constant heating power are basically equal to that of periodic alternating power with the same average power. Hack *et al*. [12] investigated the high-temperature heat pipes with a ceramic container consisting out of sintered silicon carbide and with zinc as working fluid. The results show that the best performance is reached with a filling amount of 100 g zinc as working fluid, which comes up to a filling height of about 11% of the total heat pipe length under liquid conditions.

At the same time, the life of heat pipe is a hot topic in the research of heat pipe. In many heat pipe experiments, researchers found that the generation of non-condensable gas (NCG) in the heat pipe is considered as one of the main factors affecting the life of heat pipe [13]. The researchers found that the existence of a certain amount of NCG is helpful to the start-up stage of high-temperature heat pipe. Ochterbeck *et al*. [14] investigated the effect of NCG on the start-up of heat pipe by establishing a 1-D transient model. The freezing start-up of high-temperature heat pipe becomes easier after adding non condensable gas. However, the existence of NCG may cause the start-up difficulty or failure of the loop heat pipe [15]. By using the characteristic of NCG affecting the thermal resistance of high-temperature heat pipe, a variable heat conduction heat pipe can be made [16], or the working temperature of LHP can be actively and accurately controlled [17]. However, the specific effect of NCG on the heat transfer performance of high-temperature heat pipe is still relatively small, which has a more important reference role for the application design and performance optimization of high-temperature heat pipe [16, 18].

Experimental system

The experimental system consists of four parts: heating equipment, high-temperature heat pipe, temperature measurement, and recording output system. Test system diagram and thermocouple measuring point layout are shown in fig. 1.

The working fluid of high-temperature heat pipe is sodium, and the fill volume is 175 g. The specific parameters of heat pipe are shown in tab. 1. A series of *K*-type thermo-

couples are arranged in the axial direction of the heat pipe to measure the temperature of the high-temperature heat pipe. The location of the thermocouple measuring points is shown in Fig. 1. The temperature values of each measuring point are automatically collected and recorded by the data acquisition instrument.

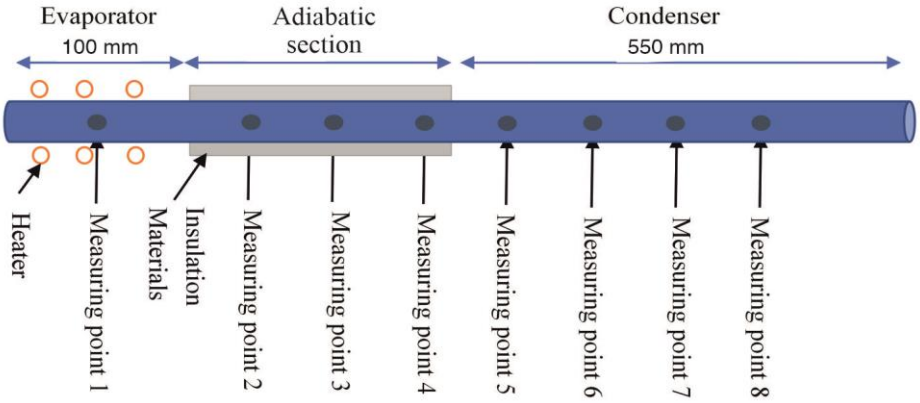

Figure 1 Test system diagram and thermocouple measuring point layout

Table 1 Parameters of sodium heat pipe

Parameter	Numerical value
Heat pipe length [mm]	1000
Length of evaporation section [mm]	100
Length of insulation section [mm]	350
Length of condensing section [mm]	550
Working fluid	Sodium
Working fluid filling capacity [g]	175
Wall material	Stainless steel
Outer diameter of heat pipe [mm]	32
Inner diameter of heat pipe [mm]	28
Capillary wick	Stainless steel wire mesh

Uncertainty analysis

Reliable temperature and heat flux measurements are vital, so the uncertainty analysis is necessary. The temperature is measured by the *K*-type thermocouples and recorded by multi-channel data logger. The precision of the calibrated thermocouple is 1 °C when the maximum calibrated temperature is 1000 °C. The precision of the multi-channel data logger is 0.2%. In this study, the experimental measurement temperature is from environmental temperature 20 °C to maximum heat pipe temperature of 750 °C. Thus, the uncertainty of temperature can be culculate as:

$$\sigma_{\mathrm{t}} = \left(\sigma_{\mathrm{tc}}^2 + \sigma_{\mathrm{l}}^2\right)^{1/2} \tag{1}$$

$$\sigma_{\mathrm{tc}} = 0.1\% \tag{2}$$

$$\sigma_l = 0.2\% \tag{3}$$

where σ_t is the uncertainty of temperature, σ_l – the precision of the multi-channel data logger, and σ_{tc} – the precision of the calibrated thermocouple.

Results and discussions

For the study on the heat transfer performance of high-temperature heat pipes, typical performances such as start-up performance and temperature uniformity are usually studied. The start-up time of the heat pipe reflects the heat response speed of the heat pipe and temperature uniformity is an important manifestation of the heat transfer effect of high-temperature heat pipes.

The *flat-front startup model* is usually used to predict the startup process of high-temperature heat pipes [19]. The time from the beginning of heating to the formation of a continuous stream of steam at the outlet of the evaporation section is defined as the start-up time. Then the start-up time can be calculated by:

$$\tau = \frac{cl\left(T_{hw} - T_a\right)}{Q} \tag{4}$$

$$c = c_w + \varepsilon c_s + \left(1-\varepsilon\right)c_{ws} \tag{5}$$

where τ is the start-up time of the heat pipe, c – the heat capacity of heat pipe, l – the length of the evaporation section of the heat pipe, T_{hw} – the temperature of hot zone of heat pipe, T_a – the temperature of cold zone of heat pipe, Q – the heating power of the heat pipe, c_w – the heat capacity of the heat pipe wall, c_{ws} – the heat capacity of the wick, and ε – the porosity of capillary wick.

Effect of inclination angle on performance of high-temperature heat pipe

In the experiment, the performance of high-temperature heat pipe was tested under the same heating power (3000 W) and different inclination angles (0°, 30°, 60°, and 90°), and the results are shown in fig. 2. It shows the temperature variation of sodium heat pipe with different inclination angles. It shows the change of start-up time of heat pipe when the inclination angle of heat pipe increases from 0° to 90° in fig. 3. It can be seen from fig. 3 that the influence of inclination angle on start-up time is not very significant, and the fluctuation is very small. As the inclination angle changes, the start-up time of the heat pipe does not change more than 5%. It can be seen from eq. (4) that the start-up time is related to the heat capacity and heating power of the heat pipe. When the heating power remains the same, the start-up time is determined by the heat capacity of the heat pipe. The experimental results are consistent with the prediction results of the *flat-front startup model*. This conclusion is consistent with the result in [20] that the inclination angle has little effect on the start-up time of the heat pipe.

The axial temperature distribution of heat pipe at different inclination angles is shown in fig.4. It can be seen from fig. 4 that with the increase of heat pipe inclination angle, the heat transfer performance of heat pipe first increases and then decreases, and the heat transfer performance is the best when the inclination angle is 30°. Chandrasekaran and Srinivasan [21] investigated the heat pipe with deionized water as the working fluid and the results showed that the heat pipe at an inclined position of 45° has about 71% higher heat transfer coefficient with minimum thermal resistance when compared to the horizontal and vertical positions. This difference is mainly due to the different structure of the heat pipe.

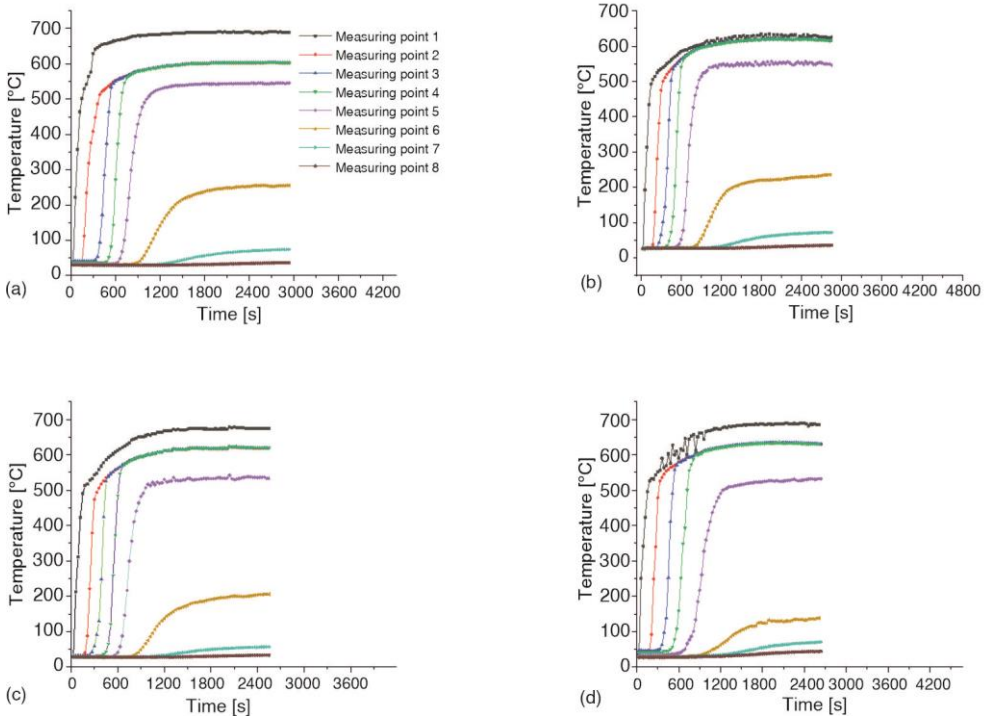

Figure 2. Temperature variation of 3000 W heat pipe with different inclination angles; (a) 0º, (b) 30º, (c) 60º, and (d) 90º

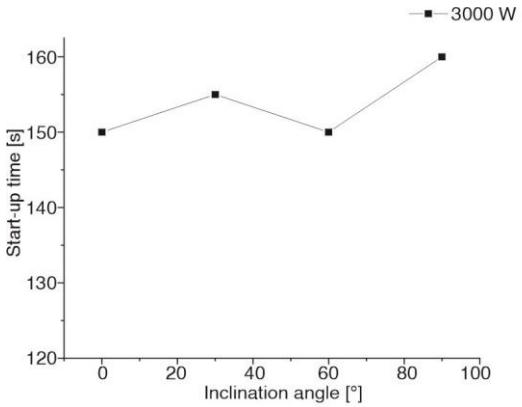

Figure 3. Start-up time chart of 3000 W heating power with different inclination angles

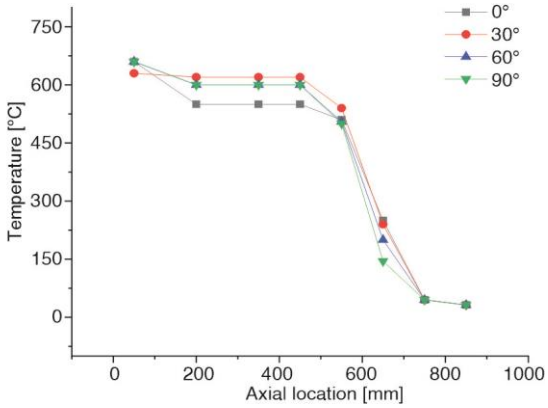

Figure 4. Axial temperature distribution of heat pipe with different inclination angles at 3000 W heating power

Influence of NCG on heat transfer performance of high-temperature heat pipe

From the axial temperature distribution diagram of high-temperature heat pipe shown in fig.4, it can be seen from fig. 4 that the heat pipe contains a certain amount of NCG, which has a certain impact on the heat transfer performance of the heat pipe. It is difficult to

completely avoid the NCG in the process of manufacturing and using the heat pipe [13]. Therefore, it is necessary to consider the influence of NCG when studying the high-temperature heat pipe. The common analysis model [22] of high-temperature heat pipe does not consider the influence of NCG.

The heat transfer model of NCG in heat pipe during steady-state operation is usually compared with circuit model [23]. The typical network model of heat pipe is shown in fig. 5 [15]. The thermal resistances are defined as the ratio between temperature differences and the heat power transferred. In this figure, R_1 and R_9 are related to the external heat exchange phenomena, R_2, R_8, and R_{10} are related to the heat conduction through the tube wall in the axial (evaporator and condenser regions) and longitudinal directions, respectively, R_3 is related to the evaporation, and has two sub regions: the pool boiling resistance and in the evaporator rear region where working fluid accumulates, and the liquid film in the wall, R_4 and R_6 are the thermal resistances associated with the interface liquid-vapor, for the evaporator and condenser, respectively, usually neglected, and finally, R_5 is the thermal resistance associated with the vapor flow inside the tube. R_7 is the condensation resistance.

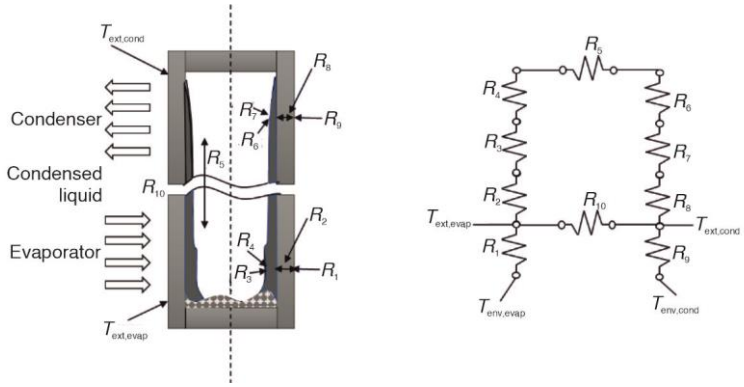

Figure 5. Typical network model of heat pipe without NCG [15]

Heat is transferred from the outer wall of evaporation section, and transferred to condensation section through axial heat conduction of heat pipe, or radial heat conduction of evaporation section, working fluid evaporation, working fluid-flow, working fluid condensation, and radial heat conduction of condensation section finally transfers to condensation section. The temperature of the outer wall of the evaporation section is $T_{ext,\ evap}$, and the temperature of the outer wall of the condensation section is $T_{ext,\ cond}$, $T_{env,\ evap}$, and $T_{env,\ cond}$ are the environment temperature. Considering the existence of NCG in the heat pipe, the model of the improved heat pipe is shown in fig.6.

After adding NCG, the condensed gas will form a NCG section at the tail end of the heat pipe under the action of steam pressure, and a certain interface thermal resistance is considered at the interface between the NCG and the condensing section. The R_{11} is the interface thermal resistance between the NCG and the wall of the heat pipe. The R_{12} is the interface thermal resistance between the NCG and the working fluid steam. It can be calculated from the area of the NCG and the interface heat transfer coefficient according to the calculation formula in the figure. The R_{13} is the heat conduction thermal resistance of the heat pipe wall in the NCG section.

It is generally believed that under the heat flux below the boiling limit of the heat pipe, the phase change of the liquid pool in the heat pipe is mainly evaporation or nucleate

boiling. But for the inside of the high-temperature heat pipe, the density of liquid metal, the viscosity and heat capacity of the working fluid are relatively large. So, it is difficult to have severe nuclear boiling. Therefore, it is assumed that the main phase transformation mode in the evaporation section is evaporation [24]. In order to simplify the calculation, the following assumptions are made: the evaporation section is full of liquid, the adiabatic section does not participate in heat transfer and the condensation section is film condensation, forming a uniform film on the pipe wall, the interface between the condensation section and NCG section is plane, and the diffusion and mass transfer between NCG and steam are not considered, as well there is natural convection heat transfer in NCG section.

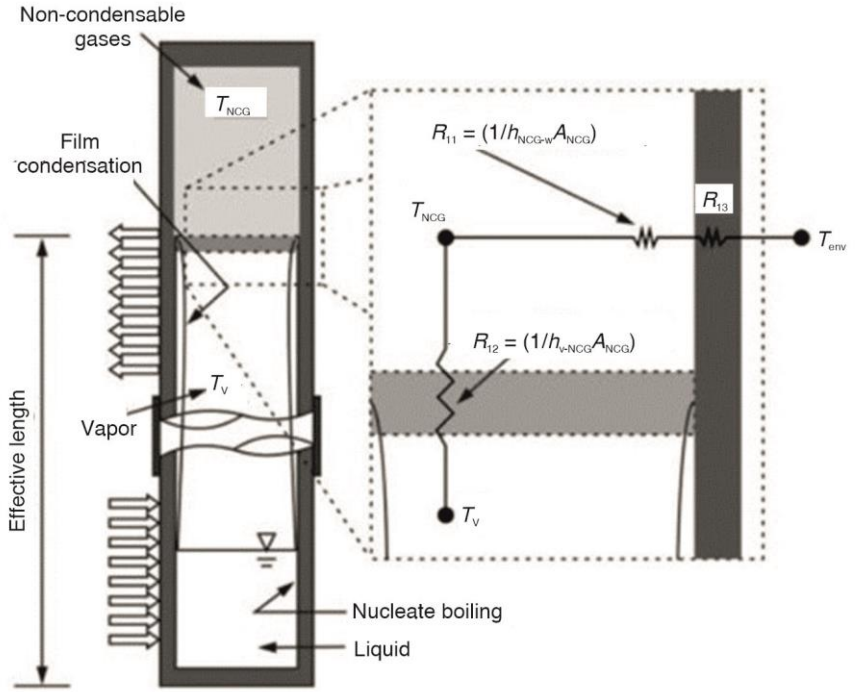

Figure 6. Heat transfer model of NCG section of heat pipe containing NCG [15]

Then the energy balance equation in part *i* can be obtained:

$$\rho_i A_i \delta_i c_{p,i} \frac{\mathrm{d}T_i}{\mathrm{d}t} = Q_{i,1} - Q_{i,2} \tag{6}$$

$$Q_{i,1} = \lambda_i A_i \frac{T_{i,1} - T_i}{\frac{\delta_i}{2}} \tag{7}$$

$$Q_{i,2} = \lambda_i A_i \frac{T_i - T_{i,2}}{\frac{\delta_i}{2}} \tag{8}$$

where ρ_i is the density of part i, A_i – the cross-sectional area of part i, δ_i – the length in the direction of heat transfer of part i, $c_{p,i}$ – the specific heat capacity at constant pressure of part i, T_i – the temperature of part i, $T_{i,1}$ – the hot end temperature in the heat transfer direction of part i, $T_{i,2}$ – the cold end temperature in the heat transfer direction of part i, t – the time, $Q_{i,1}$ – the input power of part i, $Q_{i,2}$ – the output power of part i, and λ – the thermal conductivity.

Using Newton's interpolation method to solve the simultaneous equations, the temperature distribution solution of the high temperature heat pipe containing NCG can be obtained.

The effect of NCG on effective length of the heat pipe

For the high-temperature heat pipe containing a certain amount of NCG, the steam temperature and pressure in the steam chamber of the heat pipe (except NCG section) has little change, so it is considered that the steam temperature and pressure in the steam chamber are consistent. The saturated steam pressure can be calculated from the steam temperature to get the pressure of the NCG section. According to the ideal gas calculation formula, the length calculation formula of NCG section is:

$$l_{\mathrm{NCG}} = \frac{1}{A_{\mathrm{c}}} \frac{N_0 \mathrm{R} T_{\mathrm{NCG}}}{P_{\mathrm{NCG}}} \tag{9}$$

$$l_{\mathrm{eff}} = L - l_{\mathrm{NCG}} \tag{10}$$

where L is the total length of the heat pipe, l_{NCG} – the length of the NCG section of the heat pipe, l_{eff} – the effective length of the heat pipe, N_0 – the number of moles, R = PV/nT – the gas constant, T_{NCG} – the NCG temperature, A_{c} – the tube cross section area, and P_{NCG} – the NCG pressure.

The influence of NCG on temperature distribution

For the transition section (adiabatic section, the junction of steam and NCG), the temperature distribution characteristics are similar to the eq. (11) [25]:

$$T_x = \frac{T_{\mathrm{cond}} - T_{\mathrm{NCG}}}{1 + \exp\left(\dfrac{x - x_{\mathrm{v-NCG}}}{s_{\mathrm{v-NCG}}}\right)} + \frac{T_{\mathrm{evap}} - T_{\mathrm{cond}}}{1 + \exp\left(\dfrac{x - x_{\mathrm{adiab}}}{s_{\mathrm{adiab}}}\right)} \tag{11}$$

where T_{cond}, T_{NCG}, T_{evap} are the temperatures of the condenser, NCG, and evaporator, respectively (obtained from the averages of the temperature data in these regions), x – the axial location, $x_{\mathrm{v\text{-}NCG}}$ and x_{adiab} are the positions of the interface vapour-NCG and of the adiabatic section, $s_{\mathrm{v\text{-}NCG}}$ and s_{adiab} are parameters which rule the curve inclination in the concavity change point.

The temperature distribution diagram of the high-temperature heat pipe containing NCG along the length of the tube is shown in fig. 7. The picture on the left side of fig. 7 is the actual measurement of the axial temperature distribution of the heat pipe containing NCG, and the picture on the right side is the prediction diagram of the theoretical model of the axial temperature distribution of the heat pipe containing NCG. It can be seen from fig. 7 that when the high-temperature heat pipe reaches a steady-state, three isothermal sections appear at one time along the axial temperature distribution of the heat pipe. They are the evaporation section, the condensation section and the NCG section. The temperature change from the evapo-

ration section to the condensing section is small, and the temperature from the condensing section to the NCG section is greatly reduced because there is no mass transfer and the heat transfer is solely dependent on heat conduction.

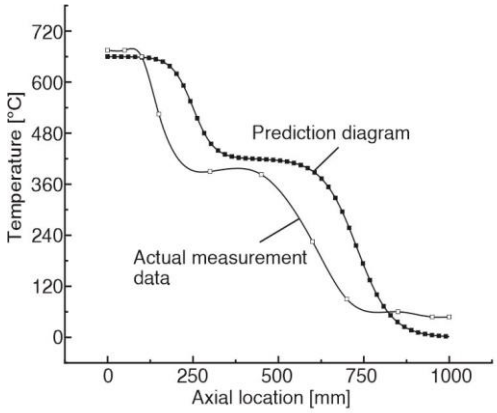

Figure 7. Temperature distribution along the length of the heat pipe containing NCG

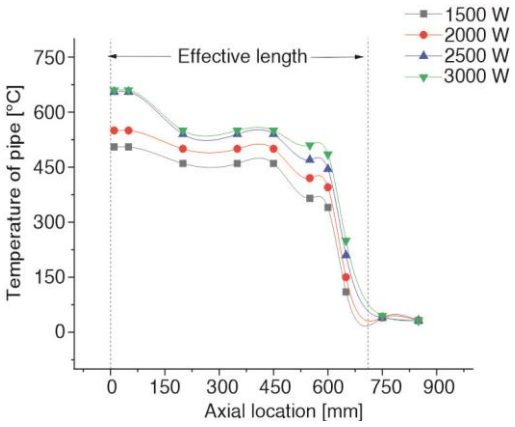

Figure 8. Fitting curve of axial temperature distribution of heat pipes with different heating power placed horizontally

In order to compare the model results with the experimental results, the axial temperature distribution of the high-temperature heat pipe under different heating powers was measured, and the results are shown in fig. 8. It is shown in fig. 8 that due to the limitation of the thermocouple measuring point arrangement and the fitting sampling setting in the experiment, some sections of the fitting curve show a wave shape. The adiabatic section is not completely insulated, so an isothermal section also appears in the adiabatic section. The approximate temperature trend is consistent with the model prediction results. The larger the input power, the closer the fitting curve is to the model prediction result. As the input power increases, the steam pressure in the heat pipe increases, the working fluid circulates faster, and the boundary between NCG and working fluid steam becomes more obvious. It is closer to the assumption that mass transfer is not performed at the interface between the NCG section and the condensing section in the model. At the same time, it can be concluded from fig. 8 that the effective length of the heat pipe is about 710 mm.

Conclusion

Through experimental research on the sodium working fluid high-temperature heat pipe, the heat transfer performance of the sodium heat pipe under different inclination angles is obtained. A heat transfer model of sodium heat pipe containing NCG was established to study the effect of NCG on the heat transfer performance of high-temperature heat pipes. The following conclusions may be made:

- The inclination angle has no effect on the startup time of high-temperature heat pipes. But when the inclination angle is about 30°, the heat pipe has the best temperature uniformity.
- The presence of the NCG will reduce the effective length of the high-temperature heat pipe, increase the thermal resistance and decrease the heat transfer performance.
- Using the sodium heat pipe heat transfer model containing NCG established in this article, the length occupied by the NCG can be judged, and the amount of NCG contained in the heat pipe can be calculated.

Acknowledgment

The supports of our research program by National Natural Science Foundation of China (No. 11802125) and Jiangsu Province Key Laboratory of Aerospace Power System (China) are greatly appreciated. We are very indebted to the anonymous reviewers for their invaluable suggestions.

Nomenclature

A – cross-sectional area of the heat pipe, [m^2]
c – heat capacity of heat pipe, [Jm^{-1}K^{-1}]
c_p – specific heat capacity at constant pressure, [JK^{-1}]
c_s – heat capacity of structure
c_w – heat capacity of the heat pipe wall, [Jm^{-1}K^{-1}]
c_{ws} – heat capacity of the wick, [Jm^{-1}K^{-1}]
h – coefficient of heat transfer, [Wm^{-2}K^{-1}]
L – length of the heat pipe, [m]
l – length of the evaporation section of the heat pipe, [m]
l_{eff} – effective length of the heat pipe, [m]
l_{NCG} – length of the NCG section of the heat pipe, [m]
N_0 – number of moles, [mol]
P_{adiab} – pressure of non -gaseous gas, [Pa]
P_{NCG} – NCG pressure, [K]
Q – heating power of the heat pipe, [W]
R – gas constant (=PV/nT), [Jmol^{-1}K^{-1}]
s_{adiab} – length of adiabatic section, [m]
$s_{v\text{-}NCG}$ – length of the transition section between steam and NCG, [m]
t – time, [s]
T_a – temperature of cold zone of heat pipe, [K]
T_{hw} – temperature of hot zone of heat pipe, [K]
T_{cond} – temperature of condensation section, [K]
T_{evap} – temperature of the evaporation section, [K]
T_{NCG} – temperature of the NCG section, [K]
x – axial location, [m]
$x_{v\text{-}NCG}$ – positions of the interface vapor-NCG
x_{adiab} – positions of the adiabatic section

Greek symbols

δ – length in the direction of heat transfer within the computing unit, [m]
ε – porosity of capillary core, [–]
λ – thermal conductivity, [Wm^{-1}K^{-1}]
ρ – density, [kgm^{-3}]
σ_l – precision of the multi-channel data logger, [–]
σ_t – uncertainty of temperature;
σ_{tc} – precision of the calibrated thermocouple, [–]
τ – start-up time of the heat pipe, [s]

References

[1] Lu, N., *et al.*, Experimental Study on Gradient Pore Size Capillary Wicks, *Heat Transfer Research, 53* (2022), 7, pp. 57-75
[2] Lu, N., *et al.*, Research Progress and Prospect of Heat Pipe Capillary Wicks, *Frontiers in Heat and Mass Transfer, 18* (2022), 24
[3] Li, J., *et al.*, Experimental Study on Evaporation-Capillary Pumping Flow in Capillary Wick and Working Fluid System, *Thermal Science, 25* (2021), 1A, pp. 367-375
[4] Werner, T. C., *et al.*, Experimental Analysis of a High Temperature Water Heat Pipe for Thermal Storage Applications, *Thermal Science and Engineering Progress, 19* (2020), 100564
[5] Xu, R., *et al.*, Testing and Modeling of the Dynamic Response Characteristics of Pulsating Heat Pipes during the Start-up Process, *Journal of Thermal Science, 28* (2018), 1, pp. 72-81
[6] Chidambaranathan, S., Rangaswamy, S., Experimental Investigation of Higher Alcohols as Self-Rewetting Fluids in Closed Loop Pulsating Heat Pipes, *Thermal Science, 25* (2021), 1B, pp. 781-790
[7] Sun, X., *et al.*, Research on Multi-Stage Heating Method of High Speed Railway Emergency Traction Battery System Based on Flat Heat Pipe, *Thermal Science, 25* (2021), 2A, pp. 1203-1215
[8] Mahdavi, M., *et al.*, Experimental Study of the Thermal Characteristics of a Heat Pipe, *Experimental Thermal and Fluid Science, 93* (2018), May, pp. 292-304
[9] Yu, P., *et al.*, Startup Performance of High-Temperature Sodium Heat Pipe with Triangular Groove Wick (in Chinese), *Journal of Nanjing TECH University, 37* (2015), 01, pp. 99-103
[10] Li, D., *et al.*, Test Study on ISO Thermal and Heat Conducting Performance of High-Temperature Heat Pipe in Solar Energy Receiver (in Chinese), *Thermal power generation, 39* (2010), 03, pp. 40-44
[11] Shen, Y., *et al.*, Heat Transfer Characteristics of High Temperature Heat Pipe with Triangular Grooved Wick Under Variable Heat Fluxes (in Chinese), *CIESC Journal, 65*. (2014), 10, pp. 3829-3837

[12] Hack, N., *et al.*, Ceramic Heat Pipes for High Temperature Application, *Energy Procedia*, *120* (2017), Aug., pp. 140-148
[13] Jiang, H., *et al.*, Effect of NCG on Performance of Two-Phase Thermal Control Devices for Spacecraft, *Spacecraft Engineering*, *23* (2014), 06, pp. 114-121
[14] Ochterbeck, J. M., Modeling of Room-Temperature Heat Pipe Startup from the Frozen State, *Journal of Thermophysics and Heat Transfer*, *11* (1997), 2, pp. 165-172
[15] Mantelli, M. B. H., *et al.*, Performance of Naphthalene Thermosyphons with NCGes – Theoretical Study and Comparison with Data, *International Journal of Heat and Mass Transfer*, *53* (2010), 17-18, pp. 3414-3428
[16] Tarau, C., *et al.*, Thermal Management System for Long-Lived Venus Landers, *Proceedings*, 9th Annual International Energy Conversion Engineering Conference, SaN Diego, Cal., USA, 2011
[17] Joung, W., *et al.*, Hydraulic Operating Temperature Control of a Loop Heat Pipe, *International Journal of Heat and Mass Transfer*, *86* (2015), July, pp. 796-808
[18] El-Genk, M., Tournier, J.-M., Challenges and Fundamentals of Modeling Heat Pipes' Startup from a Frozen State, *AIP Conference Proceedings*, *608* (2002), 1, 127
[19] Cao, Y., Faghri, A., Closed-Form Analytical Solutions of High-Temperature Heat Pipe Startup and Frozen Startup Limitation, *Journal of Heat Transfer*, *114*. (1992), 4, pp. 1028-1035
[20] Niu, T., *et al.*, Properties of High-Temperature Heat Pipe and Its Experimental (in Chinese), *Acta Aeronauticaet Astronautica Sinica*, *37* (2016), S1, pp. 59-65
[21] Chandrasekaran, S. K., Srinivasan, K., Experimental Studies on Heat Transfer Characteristics of SS304 Screen Mesh Wick Heat Pipe, *Thermal Science*, *21* (2017), Suppl. 2, pp. S497-S502
[22] Chai, B., *et al.*, Steady Numerical Analysis of Potassium Heat Pipe (in Chinese), *Atomic Energy Science and Technology*, *44* (2010), 05, pp. 553-557
[23] Groll, M., Rosler, S., Operation Principles and Performance of Heat Pipes and Closed Two-Phase Thermosyphons, *Journal of Non-Equilibrium Thermodynamics*, *17* (1992), Jan., pp. 91-151
[24] Shen, Y.,, *et al.*, Simulation and Experimental Analysis on Heat Transfer Characteristics of Alkali Metal Heat Pipe (in Chinese), *Acta Energiae Solaris Sinica*, *37* (2016), 03, pp. 644-650
[25] Hoehler, F. K., Logistic Equations in the Analysis of S-Shaped Curves, *Computers in Biology and Medicine*, *25*. (1995), 3, pp. 367-371

Paper submitted: February 7, 2022
Paper revised: August 21, 2022
Paper accepted: August 22, 2022